An update on the estimate of predictability of seasonal mean atmospheric variability using North American Multi-Model Ensemble

Bhaskar Jha, Arun Kumar & Zeng-Zhen Hu

Climate Dynamics
Observational, Theoretical and Computational Research on the Climate System

ISSN 0930-7575

Clim Dyn
DOI 10.1007/s00382-016-3217-1

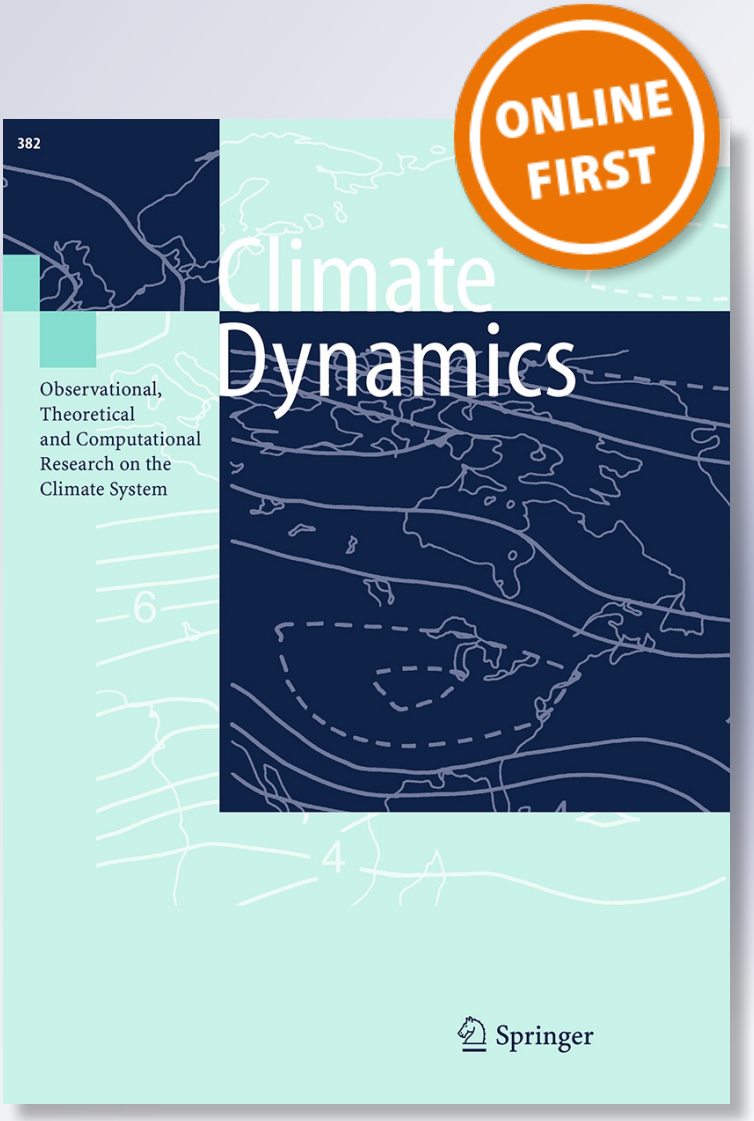

Springer

Clim Dyn
DOI 10.1007/s00382-016-3217-1

An update on the estimate of predictability of seasonal mean atmospheric variability using North American Multi-Model Ensemble

Bhaskar Jha[1,2] · **Arun Kumar**[1] · **Zeng-Zhen Hu**[1]

Received: 21 January 2016 / Accepted: 1 June 2016

Abstract In this analysis, an update in the estimate of predictable component in the wintertime seasonal variability of atmosphere documented by Kumar et al. (J Clim 20: 3888–3901, 2007) is provided. The updated estimate of seasonal predictability of 200-hPa height (Z200) was based on North American Multi-Model Ensemble (NMME) forecast system. The seasonal prediction systems participating in the NMME have gone through an evolution over a 10-year period compared to models that were used in the analysis by Kumar et al. (J Clim 20: 3888–3901, 2007). The general features in the estimates of predictable signal conform with previous results—estimates of predictability remain high in the tropical latitudes and decrease towards the extratropical latitudes; and predictability in the initialized coupled seasonal forecast systems is still primarily associated with ENSO variability. As the horizontal and vertical resolution of the models used in the current analysis is generally higher, it did not have a marked influence on the estimate of the relative amplitude of predictable component. Although the analysis indicates an increase in the estimate of predictable component, however, it maybe related to the increase in ENSO related SST variance over 1982–2000 relative to 1950–2000 (over which the analysis of Kumar et al. in J Clim 20: 3888–3901, 2007 was). The focus of the analysis is wintertime variability in Z200 and its comparison with results in Kumar et al. (J Clim 20: 3888–3901, 2007), some analyses for summertime variability in Z200, and further, for sea surface temperature, 2-m temperature and precipitation are also presented.

Keywords NMME · Predictability · Ensemble mean · 200 hPa height

1 Introduction

Predictability of seasonal mean variability principally resides in boundary condition external to atmosphere, primarily sea surface temperature (SST) associated with El Niño–Southern Oscillation (ENSO). Associated with changes in tropical heating in response to the interannual variability in ENSO SST, the resulting global response in climate variability is the underpinning of skillful seasonal predictions (Horel and Wallace 1981; Kumar and Hoerling 1995; Treenberth et al. 1998; Shukla et al. 2000; Hoerling and Kumar 2002). Skill of seasonal predictions, however, is constrained by variations in seasonal mean variabilities that are unrelated to interannual variations in external forcings. In fact, only a fraction of seasonal climate variability could be attributed to external causes that are potentially predictable (Kumar and Hoerling 1995; Barnston et al. 2005). Our attempt to quantify potential predictability of seasonal mean atmospheric variability has a long history (Madden 1976; Chervin 1986; Kumar and Hoerling 1995; Kumar

This paper is a contribution to the special collection on the North American Multi-Model Ensemble (NMME) seasonal prediction experiment. The special collection focuses on documenting the use of the NMME system database for research ranging from predictability studies, to multi-model prediction evaluation and diagnostics, to emerging applications of climate predictability for subseasonal to seasonal predictions. This special issue is coordinated by Annarita Martiotti (NOAA), Heather Archambault (NOAA), Jin Huang (NOAA), Ben Kirtman (University of Miami) and Gabriele Villarini (University of Iowa).

✉ Bhaskar Jha
Bhaskar.Jha@NOAA.GOV

[1] Climate Prediction Center, NCEP/NWS/NOAA, 5830 University Research Court, College Park, MD 20740, USA

[2] Innovim LLC, Greenbelt, MD, USA

Published online: 07 July 2016

et al. 2007; National Research Council, 2010; Delsole et al. 2013), and continues to be an area of active research.

Kumar et al. (2007) proposed a methodology to estimate the predictable and unpredictable components of the observed seasonal atmospheric variability. The method relied on a combination of observed and model simulated seasonal variability. A novel feature of the approach was use of simulations and predictions from multiple models to obtain the best estimate of predictability, and an estimate of predictability of 200 hPa heights for the December–January–February (DJF) seasonal means was presented. The analysis of Kumar et al. (2007) was based on the generation of models that were available few years prior to the completion of the analysis around 2005. The paper also commented that as seasonal prediction models improve because of advancement in models and data assimilation system, the methodology can be easily applied to obtain an improved and updated estimate of seasonal climate predictability.

In recent years, North American Multi-Model Ensemble (NMME) effort has been coordinated to improve skill of seasonal predictions (Kirtman et al. 2014; Becker et al. 2014). The NMME effort includes a collection of initialized coupled seasonal prediction systems that have been run over a common hindcast period of 1982–2010. Collectively, the seasonal prediction systems in the NMME represent an evolution of models over 10 years compared to the models that were used in Kumar et al. (2007). Further, seasonal prediction in NMME are based on coupled models, and therefore, represent a more realistic set up than model simulations used by Kumar et al. (2007) that mostly utilized AMIP simulations. In addition, NMME forecasts are initialized, and thereby, not only estimate the actual predictability but in their estimate also include possible influence of initial conditions on the predictability of seasonal mean variabilities.

The intent of the analysis presented here is to provide an update on the estimate of predictable and unpredictable components of seasonal atmospheric variability. Except for some differences outlined subsequently, the results presented here parallel the ones shown in Kumar et al. (2007), facilitating a direct comparison in updated estimates of seasonal predictability. This paper also serves as a documentation of estimate of predictability based on the current generation of seasonal prediction systems and can be repeated with the newer generation of models after a period of time.

2 Data and analysis procedure

The DJF 200 hPa mean geopotential height (Z200) hindcast used in this study are from NMME dataset (Kirtman et al. 2014; Becker et al. 2014). The DJF mean from eight seasonal prediction systems are analyzed, and depending on the model, the number of ensemble members ranges from 6 to 24 (Table 1). The analysis period extends from January 1982 to December 2010 which is the common hindcast period for all the models participating in the NMME. Some relevant details of various seasonal prediction systems in the NMME dataset, and used here, are given in Table 1. We note that different models use different start dates for their forecast initial conditions (ICs). This disparity in start dates, however, is not taken into consideration as we expect that seasonal forecast systems with shortest lead for the prediction of DJF mean variabilities will have the largest contribution from initial conditions towards predictability, and accordingly, will provide the highest estimate of predictability.

Table 1 Information about eight models' name, number of ensemble member. All model initial condition period is 1982–2010

Model	Number of ensemble member
CFSv2	24
CMC1	10
CMC2	10
GFDL	10
NASA	11
NCAR	6
GFDL_FLOR	24
NCAR_CCSM4	10
Super-Ensemble	Ensemble of 8 models (105 members)

For analyzing observed variability, the monthly Z200 from National Centers for Environmental Prediction-National Center for Atmospheric Research (NCEP–NCAR; Kalnay et al. 1996) reanalysis is used. The monthly SST data used in this analysis is the NOAA OIv2 SST analysis (Reynolds et al. 2002). ENSO variability is quantified by the Niño3.4 SST index defined as the SST anomaly averaged over (5°S–5°N, 120°–170°W). The DJF mean anomalies were computed with respect to climatology over the period of 1982–2010.

To obtain the best estimate of predictability for Z200, the analysis approach follows Kumar et al. (2007), Jha and Kumar (2009) Kumar and Hu (2014) and Kumar et al. (2016). If O_i is the observed Z200 for a particular season in the year 'i', it contains a predictable (P_i) and an unpredictable (U_i) component:

$$O_i = P_i + U_i \tag{1}$$

The predictable component could be due to interannual variations in boundary or external conditions (e.g., trends in the CO_2) or could be due to lingering influence of atmospheric initial conditions. Similarly, for the *ensemble mean* prediction from a model, if F_i is the predicted Z200 for the

same season in the year 'i'', it also made up of a predictable (E_i) and an unpredictable (S_i) components:

$$F_i = E_i + S_i \tag{2}$$

For large ensemble sizes, the unpredictable component S_i, because of ensemble averaging, approaches zero.

Assuming that predictable and unpredictable components in observations are uncorrelated, the observed variance can be decomposed as:

$$\sigma_o^2 = \sigma_p^2 + \sigma_u^2 \tag{3}$$

Here, σ_p^2 is the variance of component that can be forecast as the initial, or boundary value prediction problem, and σ_u^2 is the variance of unpredictable component. Similar to observations, the model predicted variance of ensemble mean can be decomposed as:

$$\sigma_m^2 = \sigma_{pm}^2 + \sigma_{um}^2 \tag{4}$$

Where, σ_{pm}^2 is the predictable variance related to the ensemble mean forecast, and the σ_{um}^2 is the unpredictable component. For large ensemble, the unpredictable component σ_{um}^2 approaches zero.

Physically, the unpredictable component is responsible for the dispersion among individual members within the ensemble whereby forecasts starting from small changes in IC can follow widely different trajectories (Kumar and Murtugudde 2013). Further, smaller (larger) unpredictable component relates to smaller (larger) forecast dispersion. We note that while multiple future trajectories using an ensemble of forecasts is feasible, and use of ensemble is an attempt to sample various possibilities along which observations can also evolve, observations being a single realization will only be one of those forecast trajectory.

For a particular season in the year 'i', the mean-square error (MSE) of the ensemble mean prediction is

$$MSE_i = (F_i - O_i)^2 \tag{5}$$

Under the assumption that the unpredictable components in observations and in forecast are uncorrelated, the expected value of MSE based on verification for a prediction based on a large ensemble is:

$$MSE = \sigma_u^2 + \sigma_{um}^2 + \left\langle (E_i - P_i)^2 \right\rangle \tag{6}$$

Since $\left\langle (E_i - P_i)^2 \right\rangle$ is a positive definite quantity, MSE is always larger than or equal to unpredictable component in observations, i.e., σ_u^2. If model's systematic errors for the predictable component is small, i.e., as the difference between E_i and P_i is small, and ensemble size is large, MSE converges to the unpredictable component σ_u^2. For a perfect model, $E_i = P_i$, and leads to MSE $= \sigma_u^2$. For forecast based on small ensembles, and also because of model biases in replicating the observed predictable signal, the MSE is constrained to be always larger than the unpredictable component in observations. Because various seasonal forecast systems in NMME have different ensemble size, and forecast systems have different biases, by taking the minimum value of MSE across all models we obtain the best possible estimate for the unpredictable component at every analysis grid point. Once the best estimate for the unpredictable is available, from Eq. (3) one can then estimate the predictable component as the difference between total variability for Z200 anomaly and the estimate of the unpredictable component. The signal-to-noise ratio (SNR) which is the ratio of predictable and unpredictable components is then given by:

$$\text{SNR} = \left\langle \frac{\sigma_o^2 - \text{minimum(MSE)}}{\text{minimum(MSE)}} \right\rangle^{0.5} \tag{7}$$

In the analysis we first compute the seasonal variance of observed Z200 (σ_o^2), we then calculate the MSE from each of nine models (including ensemble mean of eight individual ensembles of models). From the MSE of each model, we identify the minimum values of MSE, and then compute SNR according to Eq. (7) to obtain estimates of Z200 predictability. Although the analysis is done for every season, only the results for the DJF season are discussed.

3 Results

To provide an updated estimate of predictability, the results shown follow the same format and sequence as in Kumar et al. (2007). One difference, however, is that while the predictability estimate in Kumar et al. (2007) was based on the analysis over 1950–2000 periods, in the present analysis it is based on 1982–2010 period.

We start our discussion by showing the total variance of the observed and model forecast Z200. For different models, the total variance is computed based on individual forecast of Z200 anomalies within the forecast ensemble for DJF season initiated in November. Figure 1 shows that general features of the spatial variations in the observed variability are well captured by most models. This includes—minimum variability in the tropical latitudes; larger variability in the extratropical latitudes; in the northern hemisphere, centers with large variability over Aleutian and Greenland. Beyond the general similarities there are also some differences particularly an underestimation in the amplitude of observed variability over Greenland associated with the North Atlantic Oscillation (NAO). CFSv2, CMC1, GFDL and NCAR prediction system also

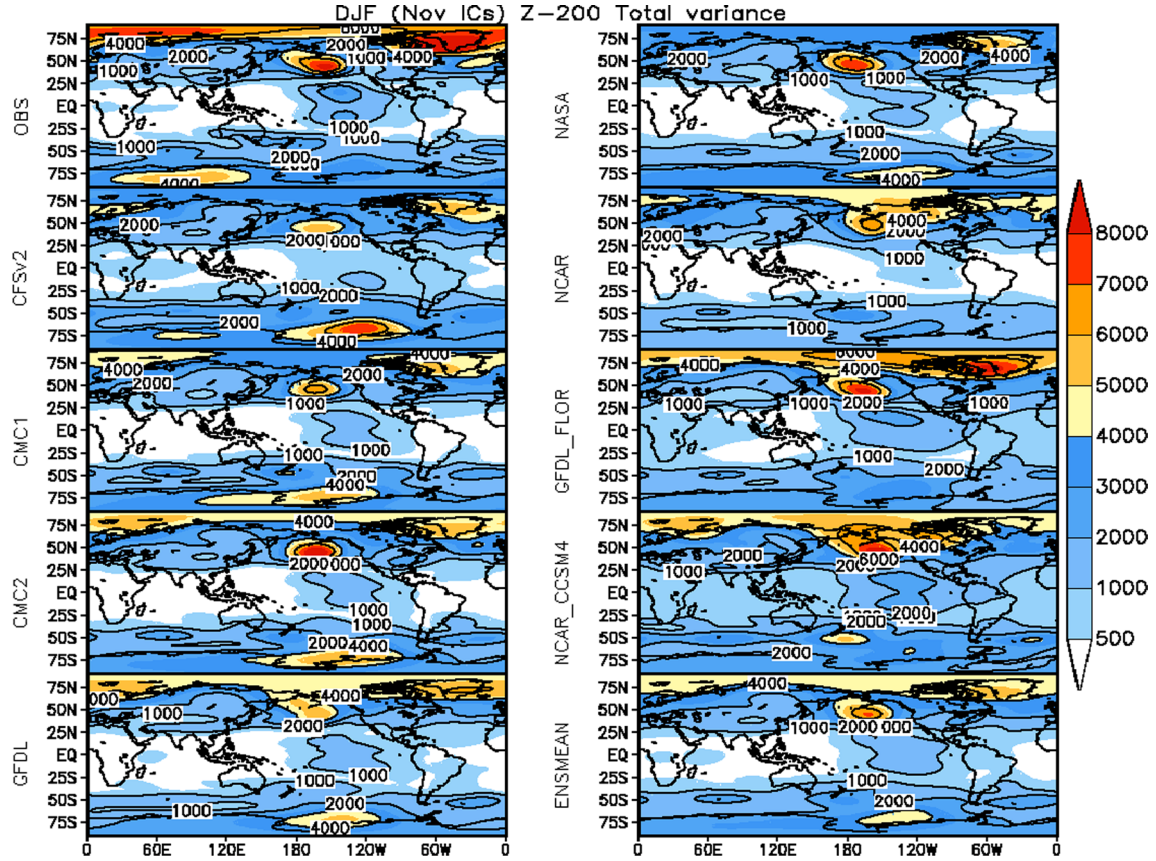

Fig. 1 Total variance for DJF seasonal means of Z200 for observations, different models and ensemble average of ensemble mean of individual eight models during 1982–2010. Unit is m^2

have weak variability over Pacific and North America, northern and southern higher latitude. There are also differences in variability over the Arctic region, for example, CFSv2, CMC1 and NASA prediction systems have weaker variability compared to the observations. As the comparison is only for the total variability, the biases in the model could be either due to errors in the predictable or the unpredictable component.

The ensemble means forecast variability (or the model's estimate of predictable component) is shown in Fig. 2. Here, the ensemble mean of each model is computed first, and then the variance of ensemble mean is calculated. In the initialized prediction, predictable signal of the atmosphere could be related to multiple factors, although as the figure shown it is dominated by the SST related forcing. In general, the spatial structure of the ensemble mean variance is consistent with the atmospheric response to El Niño–Southern Oscillation (ENSO) (Treenberth et al. 1998) across different models and highlights the dominant contribution of ENSO to the predictable signal. The amplitude of variance varies with model because of different model biases, which influence the atmospheric response to predicted SSTs. Another contributing factor is the influence of ensemble sizes and models with small ensemble size are more likely to be influenced more by the contribution of the internal variability.

The total variance of observed Z200 is shown in Fig. 3 and replicates what is shown in Fig. 1. We are interested in decomposing the total variability into components related to predictable and unpredictable variability. Although this could be done for model simulations based on the availability of ensembles, as discussed earlier, model estimates can be biased. Our goal is to obtain the best estimate of decomposition for the observed variability based on a collection of seasonal forecast systems that are likely to differ in their biases.

For each model, we next compute the MSE as defined in Eq. 4. Figure 4 shows the MSE for each model, and with the caveat that these estimates are influenced by biases in the predictable signal, and are different estimates for the observed seasonal internal variability (or the unpredictable signal) in Z200. The estimates for different model differ because of varying contribution from the model's internal variability and differences in models response to predicted SSTs. The most striking feature in the estimates of unpredictable components is that its spatial structure, by and large, is similar to the total observed variability in Fig. 3,

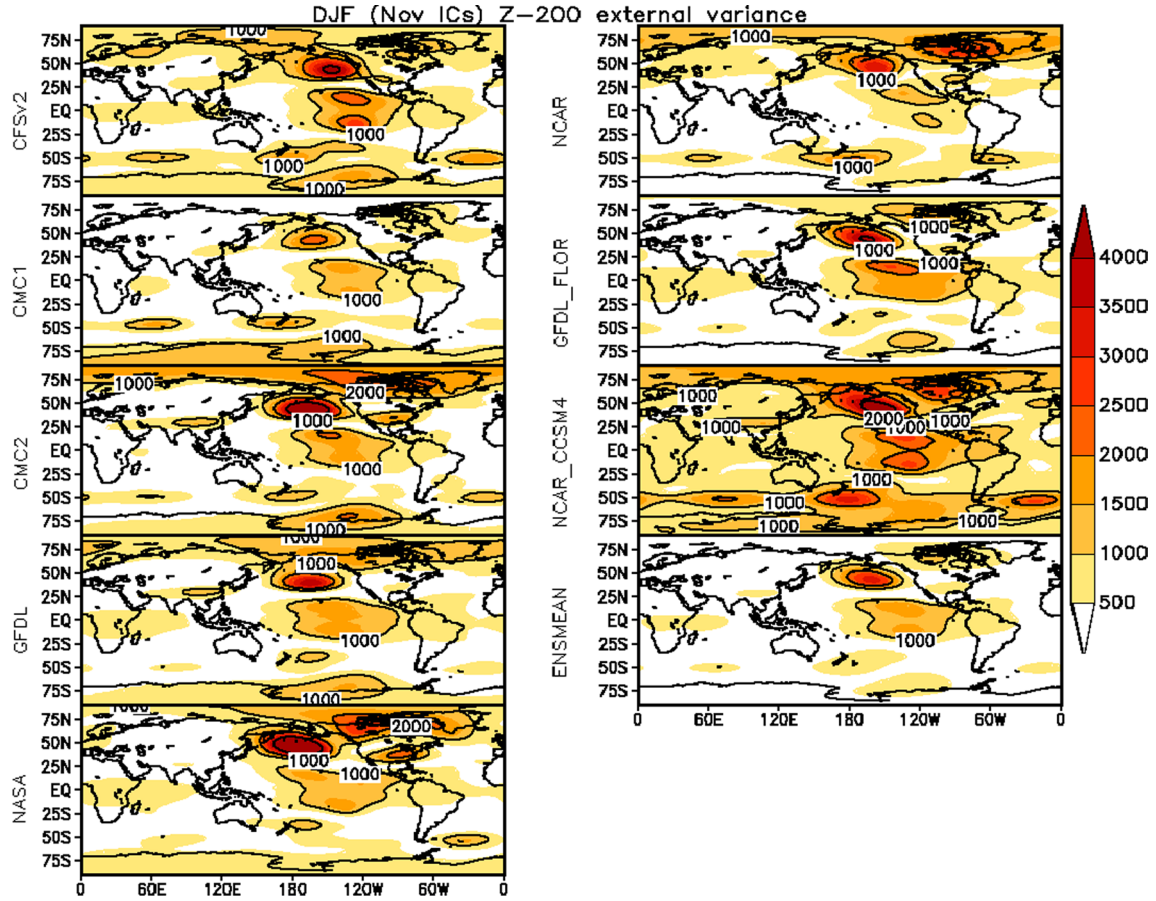

Fig. 2 Ensemble mean variance for DJF seasonal means of Z200 for different models and the average of all models during 1982–2010. IC is November and unit is m^2

and is to be expected as the estimate of predictable component (Fig. 3) is much smaller.

To get the best estimate of the unpredictable component in observations, we next find the minimum value of MSE among all the models at each grid point. Based on the MSE in the nine models (Fig. 4), the grid point-by-grid point minimum value among all the models is identified and shown in Fig. 5 (top panel) and this spatial map is our best estimate *for the unpredictable component of the observed DJF seasonal mean Z200*. Figure 5 (bottom panel) with shaded region shows the minimum value of MSE which is significant at 95 % confidence level based on the Monte Carlo test (for computational details see Kumar et al. 2007).

Once the best estimate of seasonal internal variability of Z200 is computed (Fig. 5 top panel), we estimate the predictable component by subtracting the total variance (Fig. 3) from the estimate of the unpredictable component in Fig. 5. This is shown in Fig. 6 (top panel). To compare the model based estimate of the predictable component in the observations alone, another estimate of predictable component is also computed and is based on the estimate of observed Z200 that is linearly associated with observed Niño3.4 SST variability (Fig. 6 bottom panel). Possible reasons for difference between these two estimates are the following: model based estimate includes contribution due to possible non-linearity in Z200 response to Niño3.4 SSTs, and further, due to contribution of other external factors that might influence predictability, e.g., SSTs other than those related to ENSO or soil moisture or sea ice anomalies. Model based estimate also includes possible influence from the predictability due to initial conditions. The estimate based on linear response to the Niño3.4 SST index strictly speaking, on the other hand, is an estimate of *potential* predictability as the perfect knowledge for the observed Niño3.4 SSTs during DJF is assumed. This, however, may not be a large factor having a positive influence as skill of DJF prediction of Niño3.4 SST index for forecasts starting in November is generally very high (Barnston et al. 2012). e.g., anomaly correlation exceeding 0.9.

Beside all the caveats that could lead to differences in these two estimates, there is a remarkable degree of spatial

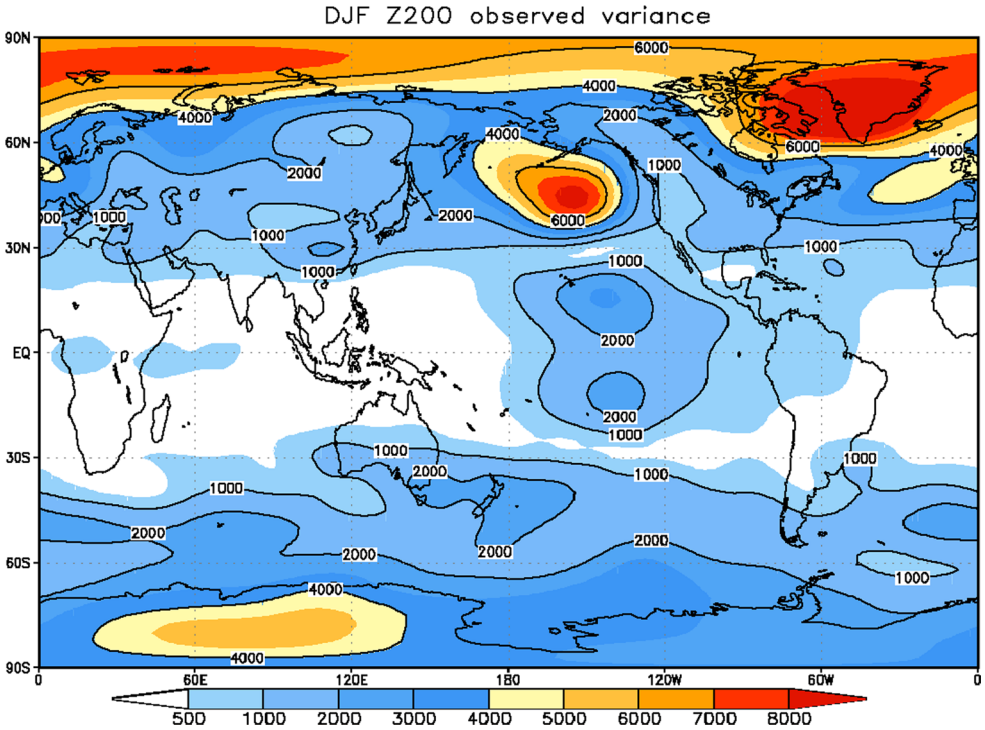

Fig. 3 Variance of the observed DJF seasonal mean Z200 anomalies for the period of 1982–2010

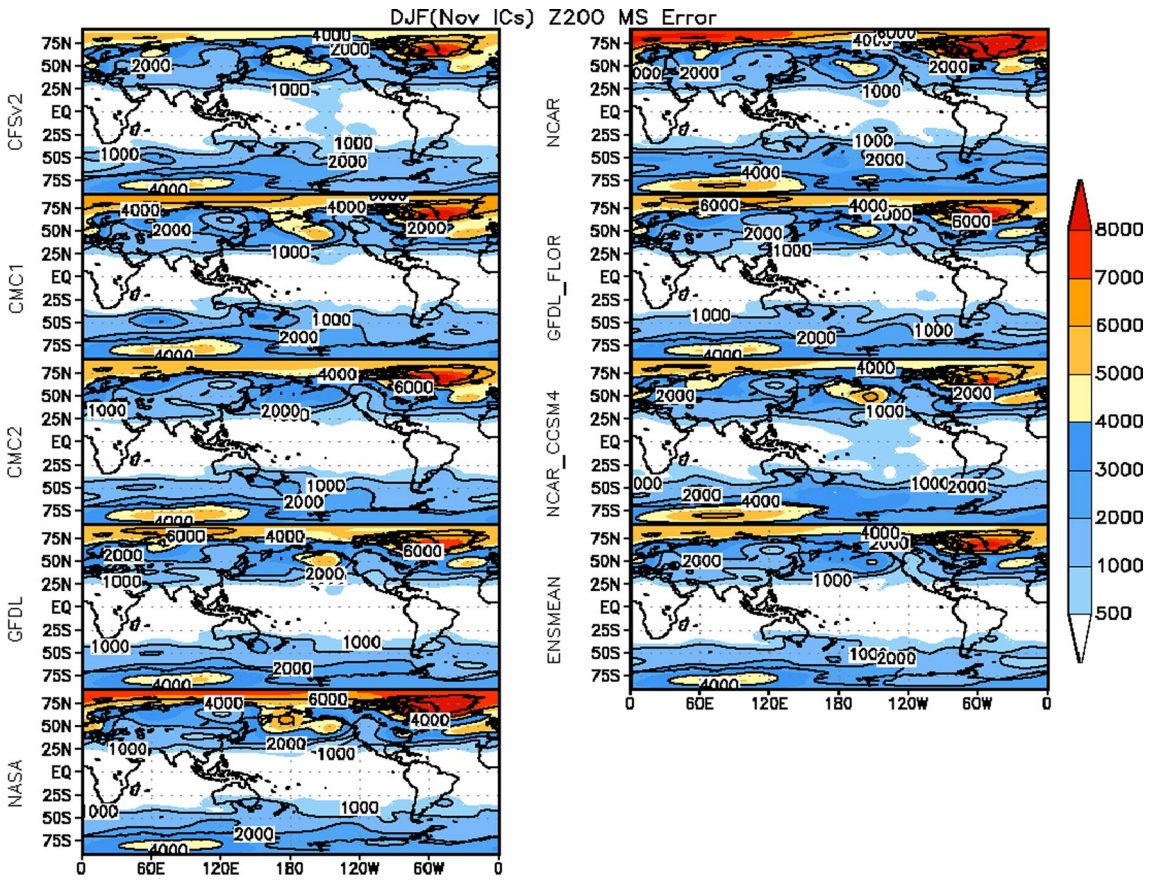

Fig. 4 MSE of the seasonal mean DJF Z200 for different models during 1982–2010. Unit is m^2

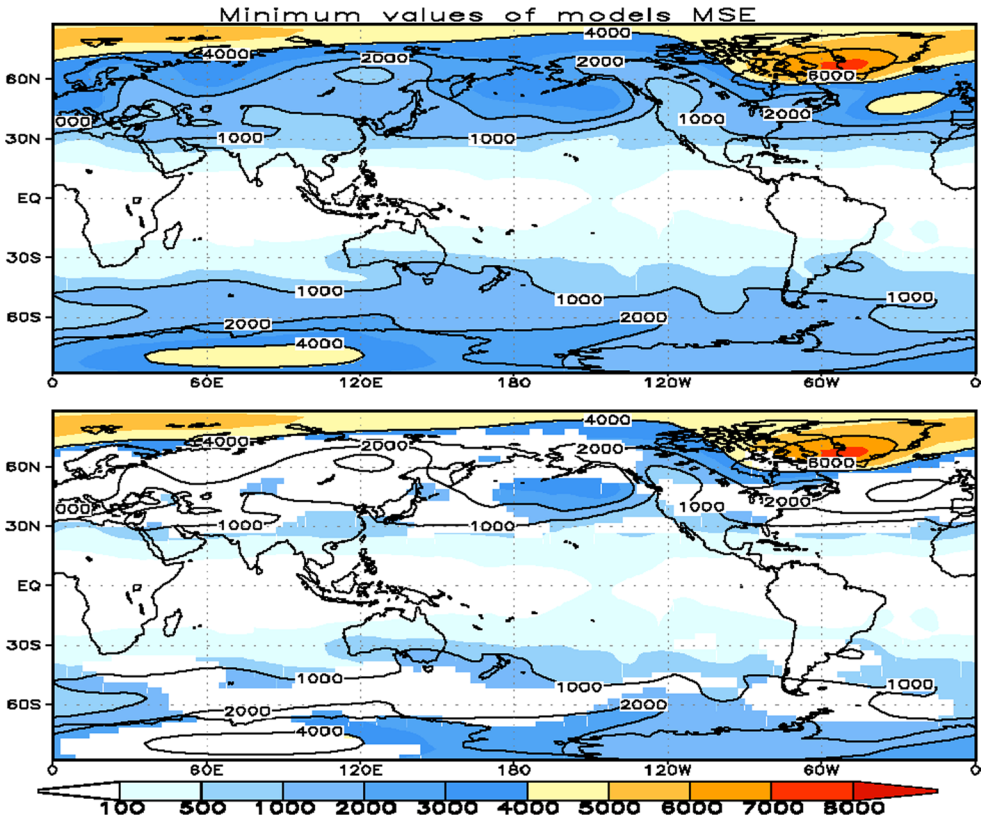

Fig. 5 (*Top*) Best estimate of the internal variance of the observed DJF Z200. The best estimate is obtained from grid-by-grid point minimum values of MSE for different coupled models. *Bottom* is same plot with shading that is the estimated MSE significant at 95 % levels based on Monte Carlo approach. Unit is m^2

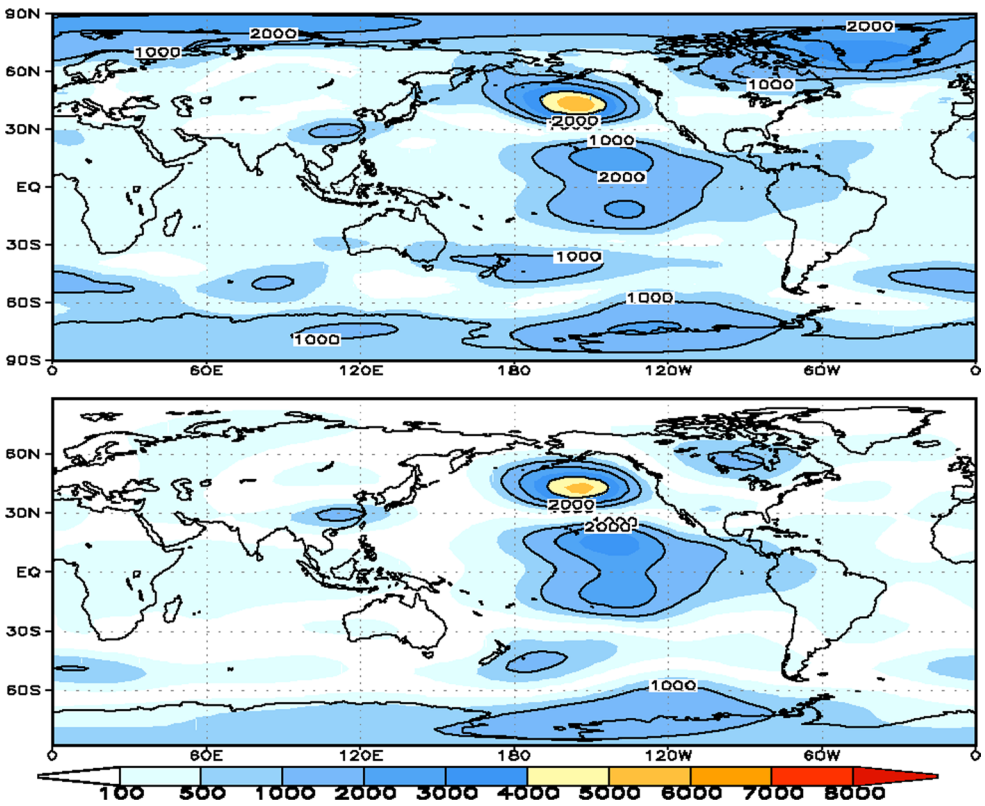

Fig. 6 (*Top*) The best estimate of external variance of the observed Z200 obtained by total variance (Fig. 3) minus best estimate of internal variance (Fig. 5). (*Bottom*) observed DJF Z200 variance linearly related to Niño3.4 SST index. Unit is m^2

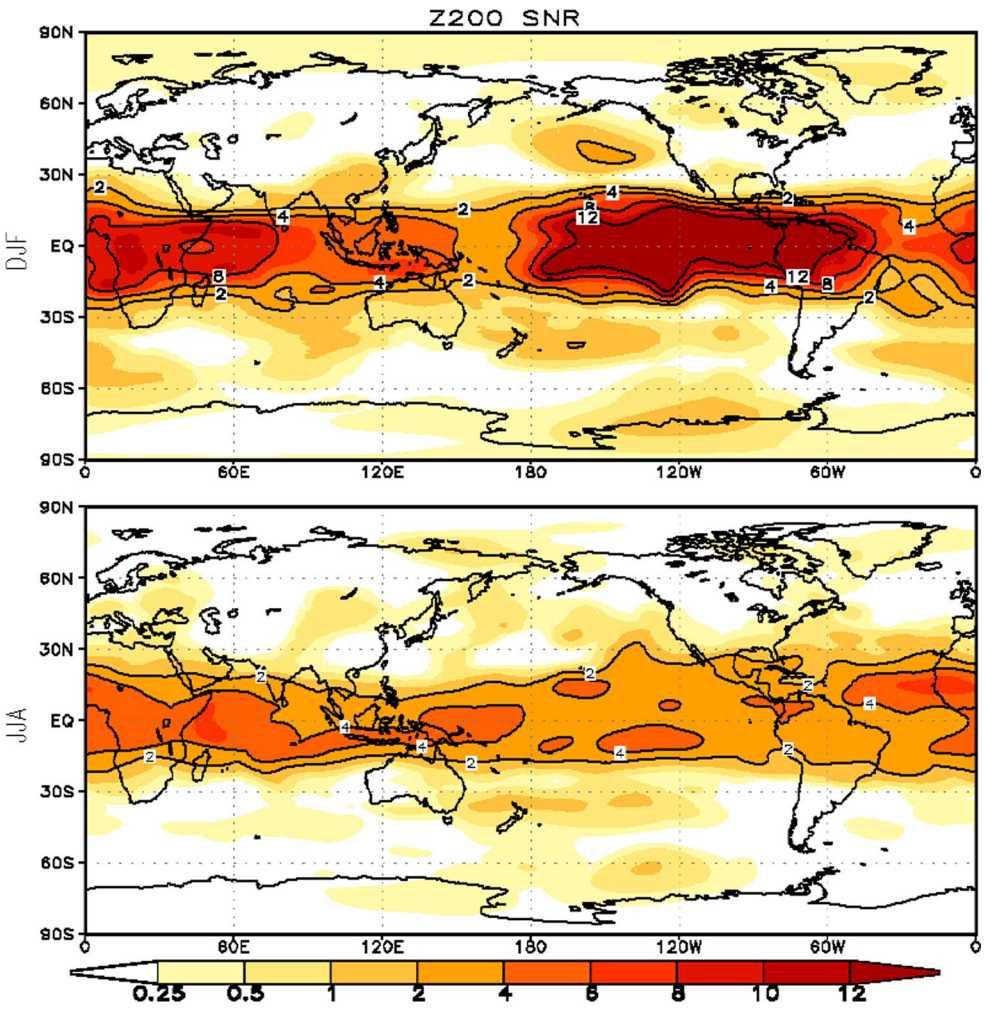

Fig. 7 (*top panel*) SNR estimate for the DJF seasonal mean Z200 computed as the ratio of external-to-internal standard deviation in Fig. 6 (*top*) and Fig. 5, respectively. (*bottom panel*) same as the top panel, but for JJA. Higher ratios imply higher potential predictability

resemblance between model based and linear estimates of predictable component. This is particularly true over the region of core influence related to ENSO SST variability in the tropical and subtropical regions in the eastern Pacific extending over to the south of Aleutian Island. There are also some differences between these two estimates: In the Southern-Hemisphere the predictable component of Z200 variability shows a more uniform zonal band between 30°S and 60°S, which is not as expansive linear estimate based on Niño3.4 SST variability, and further this pattern is likely induced by the Pacific-South American pattern (Guan et al. 2014). Another large difference is over the Arctic region where model based component of predictable component is much larger. This might be due to atmospheric response to the declining sea ice (Kumar et al. 2010; Screen et al. 2014) that might be present in the model based estimate, but cannot be captured by variations in Niño3.4 SST index. A general similarity between the model based and linear estimate of the predictable component, however, suggests the dominance of ENSO influence on seasonal predictability and conforms with earlier results (Hoerling and Kumar 2002; Quan et al. 2006).

A notable feature of the predictable component is its much smaller amplitude compared to the unpredictable component and has been a recurring theme in our attempts to quantify seasonal predictability (Madden 1976; Barnett 1995; Kumar and Hoerling 1995; Stern and Miyakoda 1995; Rowell 1998; Zwiers et al. 2000; Peng et al. 2000; Straus et al. 2003; Kumar et al. 2003; Kumar et al. 2007; Delsole et al. 2013). The relative amplitude of predictable and unpredictable component can be quantified in the terms of SNR and is shown in Fig. 7 (top panel). The SNR is largest in the tropical latitudes and decreases monotonically towards the extratropical latitudes.

Although most of the discussion presented in this paper is for the analysis of winter time variability, the analysis was also done for different seasons. As an example, in Fig. 7 (bottom panel) we also show the SNR for the seasonal average of June–July–August (JJA). Compared to the SNR for DJF, SNR values for JJA are generally lower. This is to be expected as most of the seasonal atmospheric predictability is associated with interannual variations in ENSO SSTs (Fig. 6), which following the seasonal

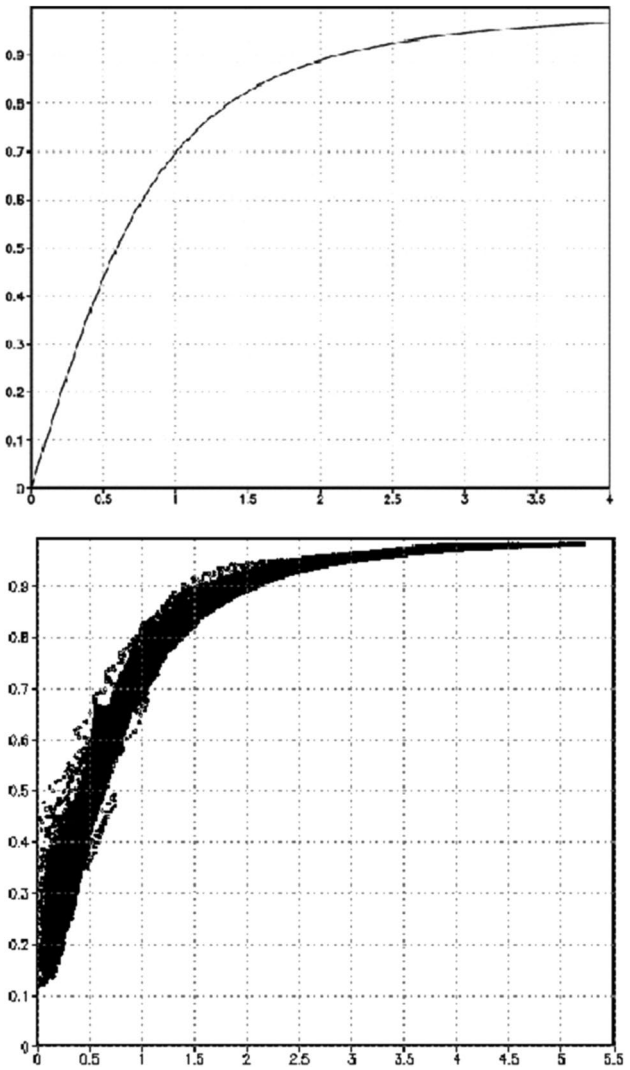

Fig. 8 (*Top*) Theoretical relationship between SNR (x-axis) and corresponding expected value of anomaly correlation (AC; y-axis). (*Bottom*) The same relationship obtained as a scatterplot between SNR in Fig. 7 (DJF) and maximum value of the AC (not shown here)

evolution of ENSO, tends to be weaker during boreal summer compared to that in boreal winter (Treenberth et al. 1998, and also discussion in the context of Fig. 10). A weaker SST forcing during JJA also translates into a weaker SNR for JJA Z200 variability.

In general, higher the SNR means higher the skill for seasonal prediction (Kumar and Hoerling 2000; Sardeshmukh et al. 2000). The theoretical relationship between the SNR and expected value of anomaly correlation (AC) for seasonal prediction system is shown in Fig. 8 (top panel) and similar relationship can be computed for other skill metrics (Kumar et al. 2001; Kumar 2009). The expected value of AC is higher for higher SNR, and asymptotes to unity for large SNR. The theoretical results match well with the results from model forecast and is illustrated based on the scatterplot between SNR and the maximum value of AC (Fig. 8, bottom panel). Similar to the minimum value of the MSE, the maximum value of AC at each grid point is computed in the following manner: (1) at each grid point, the temporal AC is computed between the ensemble mean of forecasts and observed Z200 over the analysis period. This is done for all nine seasonal prediction systems. (2) the point-by-point maximum value of AC among the nine seasonal prediction models is next identified and is used in the scatterplot in Fig. 8 (bottom panel). This procedure is similar to estimating the internal variance of Z200 by selecting the grid point by grid point minimum value of MSE. There is very close resemblance between model based analysis and theoretical relationship (up panel of Fig. 8), reconfirming the relationship between SNR and AC.

The final set of figures presents the SNR for sea surface temperature (Fig. 10), 2-m temperature (Fig. 11) and precipitation (Fig. 12). The relevance for SST is in the context of source of predictability for the atmospheric and terrestrial variables, while 2-m temperature and precipitation are variables of societal interest. The analysis for both boreal winter (top panels) and boreal summer (bottom panels) is included.

SNR for observed SST (Fig. 10) is largest in the tropical latitudes, and further, it is larger in the tropical Pacific indicating the dominance of ENSO in dictating the spatial structure in the predictability of SST. As discussed earlier, the SNR is also larger during boreal winter compared to that in boreal summer, and is because of the seasonality in the evolution of ENSO SSTs that peak in boreal winter. The contrast in the SNR during DJF and JJA is also consistent with the skill in predicting SSTs (Chen et al. 2015). Although the SNR for SSTs is lower in the extratropical ocean basins, their values are still much larger than corresponding SNR for Z200 (Fig. 7). Larger SNR values for SST in extratropical ocean compared to the Z200 is because of larger persistence for SSTs compared to the variability associated with the atmospheric variables (Kumar et al. 2011).

SNR for observed 2-m temperature, both for DJF and JJA, does not represent a coherent picture. For DJF the largest values occur in the tropical latitudes, e.g., over South America and are consistent with the seasonality of ENSO SSTs and its predictability (Fig. 10). One complicating factor in the assessment of the SNR for 2-m is the warming trends over the analysis period that, although adding to predictability, may also result in some unexpected features (in the context of their relationship with ENSO SSTs) in the spatial pattern of SNR, for example, higher values during JJA over Asia near 30°N.

SNR for observed precipitation (Fig. 12) is largest in the equatorial Pacific and conforms to its predictability to be primarily associated with ENSO SST variability (Kumar et al. 2011). Further, similar to the seasonality in the SNR

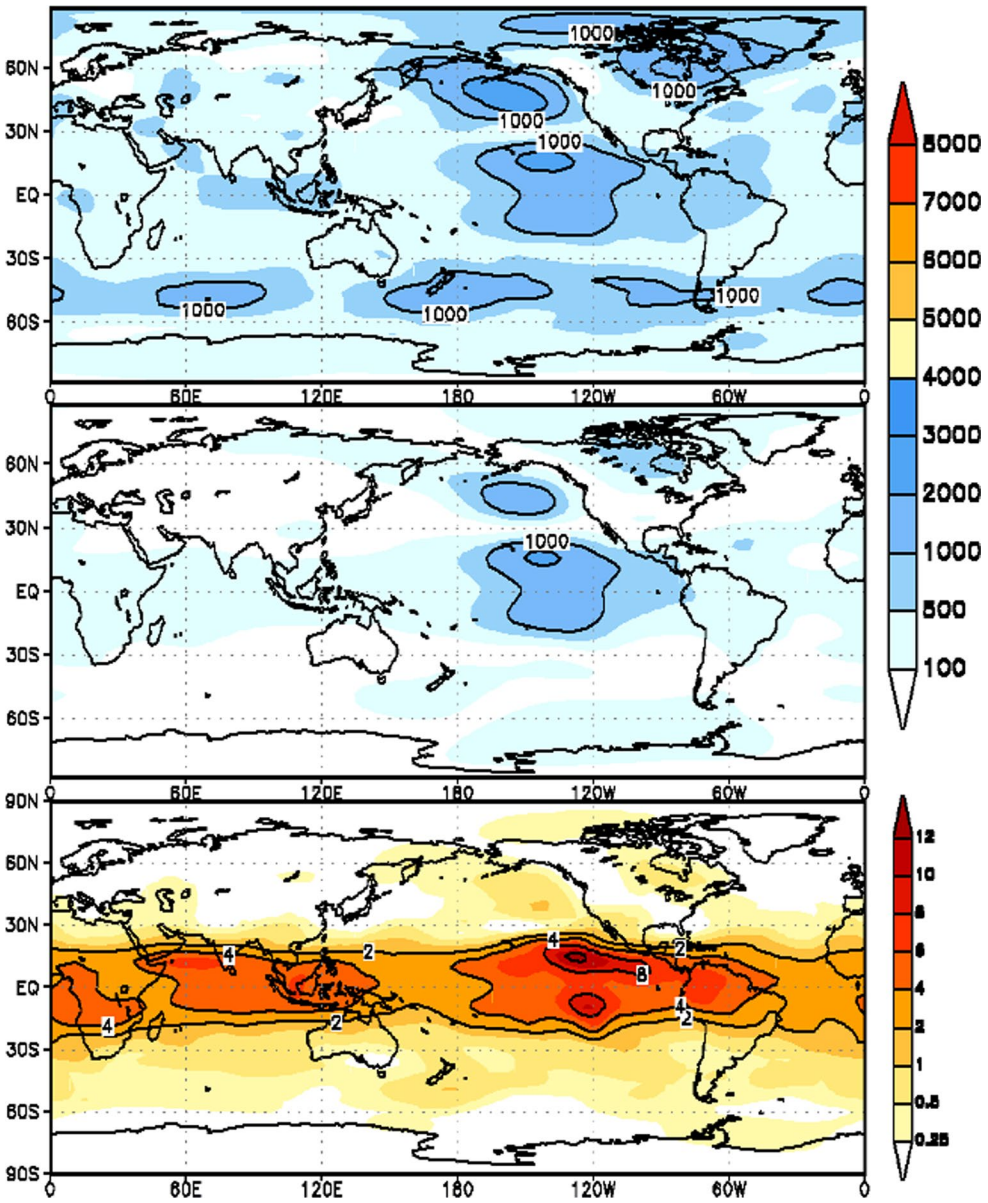

Fig. 9 The *top*, *middle*, and *bottom* panel plots are similar to Figs. 6 and 7 respectively from current analysis, but replot of Kumar et al. (2007) paper

for SST, SNR in the equatorial Pacific is generally larger in boreal winter than in boreal summer, and further, values with larger SNR have a larger spatial extent. Similar to the spatial structure in SNR for Z200, the SNR for precipitation also has a sharp decline from the tropical to extratropical latitudes, and highlights problems and limitations associated with the seasonal prediction of precipitation beyond the core regions of ENSO SST variability (Peng et al. 2000).

4 Summary and discussion

Kumar et al. (2007) provided the best estimate of predictable and unpredictable component of seasonal mean variability for the observed 200 hPa DJF heights, and their estimate was based on simulations with climate models circa 2005. The purpose of this analysis was to provide an update to the estimate of predictable and unpredictable components based on seasonal prediction systems that have gone through an evolution over a 10-year period. Figures 2, 3, 4, 5, 6, 7 and 8 in this paper corresponded to Figs. 1, 2, 3, 4, 5, 6 and 7 in Kumar et al. (2007) and facilitate a direct comparison, however, with bearing the caveat in mind that the analysis periods differ.

A comparison of predictability estimate done 10 years apart does not show marked differences, particularly over the extratropical latitudes. Estimates of predictability remain high in the tropical latitudes and decrease towards the extratropical latitudes. Predictability in the initialized coupled seasonal forecast systems is still primarily associated with ENSO variability. As the horizontal and vertical resolution of the models

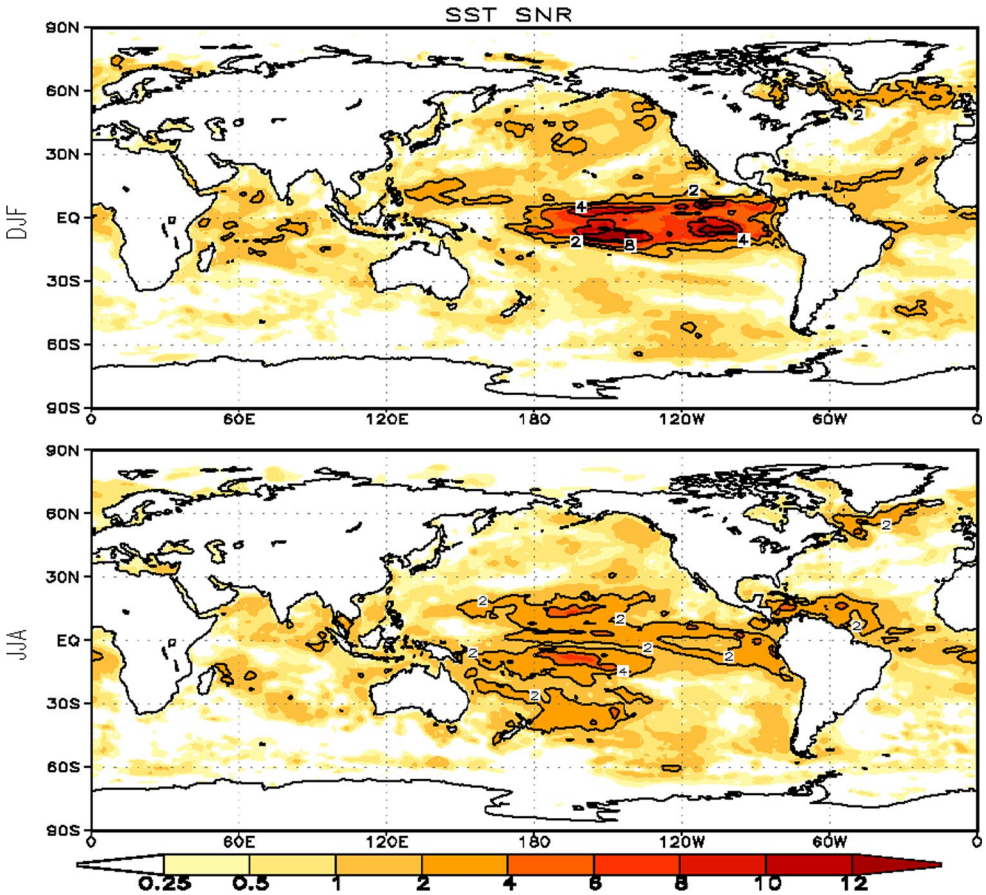

Fig. 10 Same as Fig. 7 but for sea surface temperature

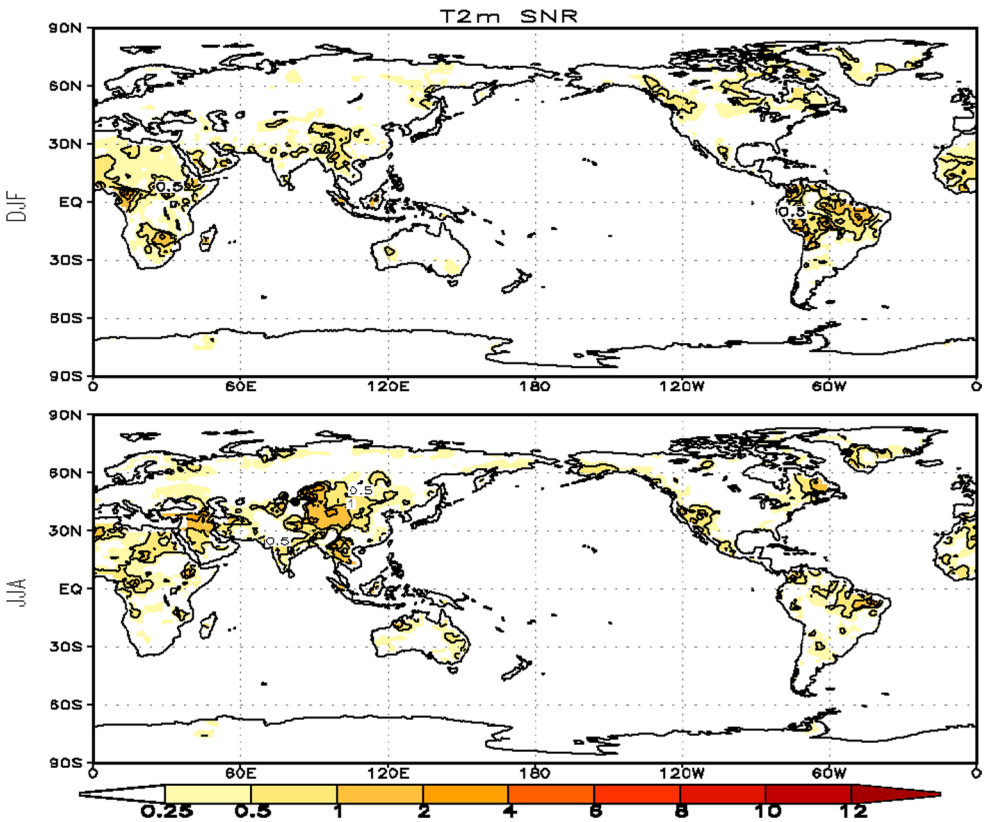

Fig. 11 Same as Fig. 7 but for seasonal mean 2-m temperature

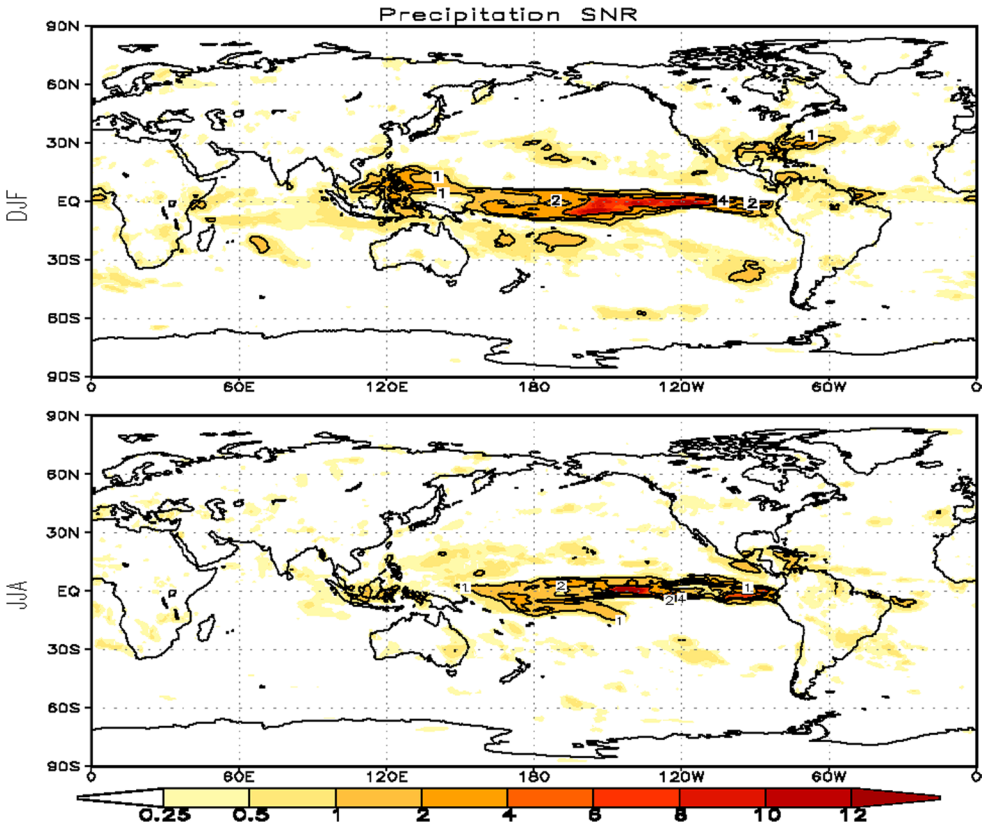

Fig. 12 Same as Fig. 7 but for seasonal mean precipitation

used in the current analysis is generally higher, this also did not lead to a marked change in the estimate of the relative amplitude of predictable component. There are some differences in the estimate, however, and are next discussed.

For the ease of comparison with Kumar et al. (2007), salient results from their analysis are included in Fig. 9 and show (1) model and Niño3.4 estimated predictable variance (and correspond to two panels in Fig. 6), and (2) SNR (that corresponds to Fig. 7). Although the most striking feature is the spatial similarities between current and Kumar et al. (2007) results with larger values of model and Niño3.4 estimated predictable variance having a geographical preference (which is connected with teleconnections associated with ENSO SSTs), the main difference is larger values for the current analysis. An apparent increase in the predictable component, however, may not be related to improvements in seasonal forecast system over a 10 year period, but maybe is due to the difference in ENSO related SST variability over the respective analysis period. To confirm this, we compared SST variability for the DJF over 1950–2000 and 1982–2010, and indeed, found SST variability to be larger for the latter period (plots not shown). The variance for Niño3.4 SST index over 1950–2000 was 1.12 K^2 while over 1982–2010 period was 1.54 K^2. Assuming that atmospheric response to ENSO SSTs is dominantly linear (Hoerling et al. 1997; Hoerling and Kumar 2002), and increase in ENSO SST variability over 1982–2010 relative to that for 1950–2000, will also translate in an increase in predictable component.

For both the analyses, the SNR in the extratropical regions (Fig. 7, and bottom panel in Fig. 9) remains small and is indicative of the dominance of atmospheric internal variability and its contribution to the unpredictable component. As mentioned earlier, one distinct feature in the estimate of predictability (and which cannot be easily accounted for by an increase in ENSO SST variability) is over the Arctic region, and could be due to a response to sea ice decline (Kumar et al. 2010; Screen et al. 2014). Overall, this analysis provided an update in the estimate of predictability and unpredictable component of DJF 200 hPa seasonal variability based on the current generation of seasonal predication system. We envision that similar updates will be generated on a routine basis to (a) provide a converging estimate for seasonal predictability, and (b) document the influence of improvements in models on quantifying predictability estimates of SST, T2m, and precipitation (Figs. 10, 11, 12).

Acknowledgments The NMME project and data dissemination are supported by NOAA, NSF, NASA and DOE. The help of NCEP, IRI and NCAR personnel in creating, updating and maintaining the NMME archive is acknowledged. All the data used in this paper are available at NOAA Climate Prediction Center (CPC) (http://www.cpc.

ncep.noaa.gov/products/NMME/). The scientific results and conclusions, as well as any view or opinions expressed herein, are those of the authors and do not necessarily reflect the views of NWS, NOAA, or the Department of Commerce.

References

Barnett TP (1995) Monte Carlo climate forecasting. J Clim 8:1005–1022

Barnston AG, Kumar A, Goddard L, Hoerling MP (2005) Improving seasonal predictions practices through attribution of climate variability. Bull Am Meteorol Soc 85:59–72

Barnston AG, Tippett MK, L'Heureux ML, Li S, DeWitt DG (2012) Skill of real-time seasonal ENSO model predictions during 2002–2011—is our capability increasing? Bull Am Meteorol Soc 93(5):631–651

Becker E, van Dool Huug, Zhang Q (2014) Predictability and forecast skill in NMME. J Clim 27:5891–5906. doi:10.1175/JCLI-D13-00597.1

Chen M, Kumar A, Wang W (2015) A Study of the predictability of sea surface temperature over the tropics. Clim Dyn 44:1767–1776

Chervin RM (1986) Interannual variability and seasonal climate variability. J Atmos Sci 43:233–251

Delsole T, Kumar A, Jha B (2013) Potential seasonal predictability: comparison between empirical and dynamical model estimates. Geophys Res Lett 40:1–7

Guan Y, Zhu J, Huang B, Hu Z-Z, Kinter JL III (2014) South Pacific Ocean dipole: a predictable mode on multi-seasonal time scales. J Clim 27:1648–1658

Hoerling MP, Kumar A (2002) Atmospheric response patterns associated with tropical forcing. J Clim 8:474–495

Hoerling MP, Kumar A, Zhong M (1997) El Nino, La Nina, and the nonlinearity of their teleconnections. J Clim 10:1769–1786

Horel JD, Wallace JM (1981) Planetary-scale atmospheric phenomenon associated with the Southern Oscillation. Mon Weather Rev 109:2080–2092

Jha B, Kumar A (2009) A comparative analysis of change in the first and second moment of the PDF of seasonal means with ENSO SSTs. J Clim 22:1412–1423

Kalnay E, Kanamitsu M, Kistler R, Collins W, Deaven D, Gandin L, Iredell M, Saha S, White G, Woollen J, Zhu Y, Chelliah M, Ebisuzaki W, Higgins W, Janowiak J, Mo KC, Ropelewski C, Wang J, Leetmaa A, Reynolds R, Jenne R, Joseph D (1996) The NCEP/NCAR 40-year reanalysis project. Bull Am Meteorol Soc 77:437–471

Kirtman BP et al (2014) The North American multimodel ensemble: phase 1 seasonal-to-interannual prediction; phase-2 toward developing intraseasoanl prediction. Bull Am Meteorol Soc 95:585–601

Kumar A (2009) Finite samples and uncertainty estimates for skill measures for seasonal predictions. Mon Weather Rev 137:385–392

Kumar A, Hoerling MP (1995) Prospects and limitation of seasonal atmospheric GCM predictions. Bull Am Meteorol Soc 76:335–345

Kumar A, Hoerling MP (2000) Analysis of a conceptual model of seasonal climate variability and implications for seasonal prediction. Bull Am Meteorol Soc 81:255–264

Kumar A, Hu Z-Z (2014) How variable is the uncertainty in ENSO sea surface prediction? J Clim 27(7):2779–2788. doi:10.1175/JCLI-D-13-00576.1

Kumar A, Murtugudde R (2013) Predictability and uncertainty: a unified perspective to build a bridge from weather to climate. COSUST 5:327–333

Kumar A, Barnston AG, Hoerling MP (2001) Seasonal prediction, probabilistic verifications, and ensemble size. J Clim 14:1671–1676

Kumar A, Schubert SD, Suarez MS (2003) Variability and predictability of 200-mb seasonal mean heights during summer and winter. J Geophys Res 108:4169. doi:10.1029/2002JD002728

Kumar A, Jha B, Zhang Q, Bounoua L (2007) A new methodology for estimating the uppredictable component of seasonal atmospheric variability. J Clim 20:3888–3901

Kumar A, Perlwitz J, Eischeid J, Quan X, Xue T, Zhang T, Hoerling M, Jha B, Wang W (2010) Contribution of sea ice loss to Artic amplification. Geophys Res Lett 37:1–6

Kumar A, Chen M, Wang W (2011) An analysis of prediction skill of monthly mean climate variability. Clim Dyn 37:1119–1131

Kumar A, Hu Z-Z, Jha B, Peng P (2016) Estimating ENSO predictability: based on multi-model hindcasts. Clim Dyn. doi:10.1007/s00382-016-3060-4

Madden RA (1976) Estimates of the natural variability of time-averaged sea-level pressure. Mon Weather Rev 104:942–952

National Research Council (2010) Assessment of intraseasonal to interannual climate prediction and predictability. the National Academies Press, Washington, 192 pp., ISBN-10: 0-309-15183-X

Peng P, Kumar A, Barnston AG, Goddard L (2000) Simulation skills of the SST-forced global climate variability of the NCEP-MRF9 and Scripps-MPI ECHAM3 models. J Clim 13:3657–3679

Quan X, Hoerling M, Whitaker J, Bates G, Xu T (2006) Diagnosing sources of US seasonal forecast skill. J Clim 19:3279–3293. doi:10.1175/JCLI3789.1

Reynolds RW, Rayner NA, Smith TM, Stokes DC, Wang W (2002) An improved in situ and satellite SST analysis for climate. J Clim 15:1609–1625

Rowell DP (1998) Assessing potential predictability with an ensemble of multi-decadal GCM simulations. J Clim 11:109–120

Sardeshmukh PD, Compo GL, Penland C (2000) Changes of probability associated with El Niño. J Clim 13:4268–4286

Screen JA, Deser C, Simmonds I, Tomas R (2014) Atmospheric impacts of Arctic sea-ice loss, 1979–2009: separating forced change from atmospheric internal variability. Clim Dyn 43:333–344

Shukla J et al (2000) Dynamical seasonal prediction. Bull Am Meteorol Soc 81:2593–2606

Stern W, Miyakoda K (1995) Feasibility of seasonal forecasts inferred from multiple GCM simulations. J Clim 8:1071–1085

Straus D, Shukla J, Paolino D, Schubert S, Suarez M, Pegion P, Kumar A (2003) Predictability of the seasonal mean atmospheric circulation during autumn, winter, and spring. J Clim 16:3629–3649

Treenberth KE, Branstator GW, Karoly D, Kumar A, Lau N-C, Ropelewski C (1998) Progress during TOGA in understanding and modeling global teleconnections associated with tropical sea surface temperature. J Geophys Res 103(7):14291–14324

Zwiers FW, Wang XL, Sheng J (2000) Effects of specifying bottom boundary conditions in an ensemble of atmospheric GGCM simulations. J Geophys Res 105:7295–7316